Incoherently coupled steady-state soliton pairs in biased photorefractive-photovoltaic materials

Lu Keqing,[1,2,3,*] Zhang Yanpeng,[2,†] Tang Tiantong,[2] and Li Bo[1]
[1]Department of Applied Physics, Xidian University, Xi'an 710071, China
[2]Department of Electronic Science and Technology, Xi'an Jiaotong University, Xi'an 710049, China
[3]State Key Laboratory of Transient Optics Technology, Xi'an Institute of Optics and Precision Mechanics, Xi'an 710068, China
(Received 13 December 2000; revised manuscript received 21 June 2001; published 12 October 2001)

A theory on incoherently coupled soliton pairs for photorefractive screening solitons is developed that gives rise to incoherently coupled steady-state soliton pairs and multicomponent spatial solitons in biased photorefractive-photovoltaic materials, which result from both the bulk photovoltaic effect and the spatially nonuniform screening of the external bias field. When the bulk photovoltaic effect is neglectable, these soliton pairs are the previously studied soliton pairs for screening solitons, these multicomponent spatial solitons predict incoherently coupled multicomponent spatial solitons for screening solitons, and their space-charge field is the space-charge field of screening solitons. When the external field is absent, these soliton pairs and multicomponent spatial solitons predict incoherently coupled soliton pairs and multicomponent spatial solitons for photovoltaic solitons, and their space-charge field is the space-charge field of photovoltaic solitons. The stability of these soliton pairs and multicomponent spatial solitons is also discussed using the modulation instability theory.

DOI: 10.1103/PhysRevE.64.056603 PACS number(s): 42.65.Tg, 42.65.Hw, 42.65.Jx, 72.40.+w

Photorefractive (PR) spatial solitons [1–22,26–29] have been investigated extensively in the past few years. At present, three different types of PR solitons have been considered in the literature. The first kind involves the so-called quasi-steady solitons [1–3], which arise when diffraction is exactly balanced by PR two-ware mixing phase coupling. The other two types, better known as screening [4–9] and photovoltaic [10–17] (PV) solitons, are possible under steady-state conditions. In particular, PV steady-state planar solitons can be supported in PR materials with appreciable PV coefficients, which result from the bulk PV effect. On the other hand, screening solitons require the application of an external bias field in photorefractive-nonphotovoltaic materials, which result from nonuniform screening of the external field. Very recently, vector solitons have also been predicted for photorefractive screening solitons, which involve the two polarization components of an optical beam that are orthogonal to one another [18,19]. Depending on the symmetry class of the appropriate crystal and its orientation, these solitary beams were found to obey a self-coupled or a cross coupled system of nonlinear evolution equations. Subsequently, incoherently coupled soliton pairs were proposed for photorefractive screening solitons [20], which involve the two beams that are incoherent with respect to each other, and soon thereafter demonstrated experimentally [21,22]. Moreover, incoherent solitons are demonstrated, both theoretically and experimentally, in noninstantaneous nonlinear media, which are multicomponent solitons that are made up from modal constituents that are incoherent with one another [23]. Finally, multicomponent composite solitons are addressed in noninstantaneous nonlinear media, which involve components that are mutually incoherent [24–26]. However, we should also pay attention to vector solitons and soliton pairs in biased photorefractive-photovoltaic materials, and multicomponent composite solitons for photorefrative spatial solitons.

More recently, we have shown theoretically that the application of an external field enables steady-state spatial solitons [27–29] in photorefractive-photovoltaic crystals, which are known as screening-photovoltaic (SP) solitons that result from both the bulk PV effect and the spatially nonuniform screening of the external bias field. Of particular interest are SP solitons which change into screening solitons when the bulk PV effect can be neglected, and PV solitons when the external field is absent. However, when the external field is absent, $I=I_d u(\hat{\xi})$ (I is the power density profile of the light beam, and I_d is the so-called dark irradiance) [13] and the space-charge field E in Ref. [21], yields $\hat{E}=(u_\infty^2-u^2)/(1+u^2)$, where $\hat{E}=E/E_p$ and $u_\infty=u(\hat{\xi}\to\infty)$. In this case, if we let $\hat{J}=u_\infty^2$, then $\hat{E}=(\hat{J}-u^2)/(1+u^2)$ has the same dimensionless parameters and form as Eq. (13) for the closed circuit ($\hat{J}\neq 0$) condition in Ref. [13]; however, $\hat{E}=(\hat{J}-u^2)/(1+u^2)$ is different from Eq. (13) for the open circuit ($\hat{J}=0$) condition in Ref. [13] because $u_\infty^2\neq 0$. The absence of the external field signifies either an open circuit or closed circuit in the absence of the external field. On the other hand, when the external field is absent, the physical system of SP solitons becomes the physical system of previously studied PV solitons [29]. Thus, when the external field is absent, the space-charge field of SP solitons ought to become the space-charge field of PV solitons in either closed-circuit or open-circuit conditions.

In this article, we obtained accurately the space-charge field of screening-photovoltaic solitons. When the bulk PV effect is neglectable, it is the space-charge field of screening solitons. When the external field is absent, it is the space-charge field of PV solitons. We show theoretically that an alternate type of the incoherently coupled soliton pairs and multicomponent spatial solitons are possible in biased

*Electronic address: kg.lu@263.net
†Electronic address: yp.zhang@263.net

photorefractive-photovoltaic crystals under steady-state conditions, which result from both the bulk PV effect and the spatially nonuniform screening of the external bias field. These soliton pairs and multicomponent spatial solitons are formed provided that the carrier beams share the same polarization, and wavelength, and are mutually incoherent. We discuss the stability of these soliton pairs and multicomponent spatial solitons by using the modulation instability theory. Finally, we find that when the bulk PV effect is neglectable, these soliton pairs are soliton pairs for screening solitons, and these multicomponent spatial solitons predict incoherently coupled multicomponent spatial solitons for screening solitons, and that when the external field is absent, these soliton pairs and multicomponent spatial solitons predict incoherently coupled soliton pairs and multicomponent spatial solitons for photovoltaic solitons.

To start, let us consider two optical beams $\mathbf{E}_1$ and $\mathbf{E}_2$ of the same frequency but mutually incoherent that propagate in a photorefractive-photovoltaic material along the z axis and are allowed to diffract only along the x direction. For demonstration purposes, let the photorefractive-photovoltaic crystal be $LiNbO_3$ with its optical c axis oriented in the x direction. Moreover, let us assume that the external bias electric field is applied in the x direction. Under these conditions, the perturbed refractive index for both beams (along the x axis) is given by $n_e'^2 = n_e^2 - n_e^4 r_{33} E$ [5,20], where n_e is the unperturbed extraordinary index of refraction, r_{33} is the electro-optic coefficient, and $\mathbf{E} = E\mathbf{i}$ is the space-charge field induced in this photorefractive-photovoltaic crystal, $\mathbf{i}$ is the unit vector pointing to the x direction. On the other hand, the total electric-field component $\mathbf{E} = \mathbf{E}_1 + \mathbf{E}_2$ of the two beams satisfies the Helmholtz equation

$$\nabla^2 \mathbf{E} + (k_0 n_e')\mathbf{E} = \mathbf{0}, \tag{1}$$

where $k_0 = 2\pi/\lambda_0$ and λ_0 is the common free-space wavelength. The optical fields are expressed as usual in terms of slowly varying envelopes (ϕ, ψ), that is $\mathbf{E}_1 = \mathbf{i}\phi(x,z)\exp(ikz)$ and $\mathbf{E}_2 = \mathbf{i}\psi(x,z)\exp(ikz)$, $k = k_0 n_e$ is the propagation constant. Substituting these forms of $\mathbf{E}_1$ and $\mathbf{E}_2$ into Eq. (1) yields the following evolution equations

$$i\phi_z + \frac{1}{2k}\phi_{xx} - \frac{k_0(n_e^3 r_{33} E)}{2}\phi = 0, \tag{2}$$

$$i\psi_z + \frac{1}{2k}\psi_{xx} - \frac{k_0(n_e^3 r_{33} E)}{2}\psi = 0, \tag{3}$$

where $\phi_z = \partial\phi/\partial z$, etc. Moreover, the induced space-charge field E can be obtained from the rate and continuity equations and Gauss's law in a PR medium with electrons as the sole charge carriers. In steady state and in two dimensions these equations are [4,13,29]

$$(\hat{s}I + \beta_T)(N_D - N_D^+) - \gamma n N_D^+ = 0, \tag{4}$$

$$\nabla \cdot \mathbf{J} = \nabla \cdot [e\hat{\mu} n \boldsymbol{E} + \hat{\mu} k_B T \nabla n + \kappa \hat{s}(N_D - N_D^+) I \mathbf{i}] = 0, \tag{5}$$

$$\nabla \cdot (\epsilon_0 \epsilon_r \boldsymbol{E}) = e(N_D^+ - N_A - n), \tag{6}$$

$$\epsilon = -\int_{-l/2}^{l/2} dx\, E, \tag{7}$$

where n is the electron density, N_D^+ is the density of ionized donors, N_A is the density of negatively charged acceptor, N_D is the total donor density, $\hat{s}$ is the photoexcitation cross section, γ is the recombination rate coefficient, $\boldsymbol{J} = J\boldsymbol{i}$ is the current density, β_T is the thermal excitation rate of the electrons, e is the electric charge, $\hat{\mu}$ is the electron mobility, k_B is Boltzmann's constant, T is the absolute temperature, κ is the PV constant, ϵ_r is the dielectric constant of the crystal, ϵ_0 is the permittivity of the vacuum, and ϵ is the external voltage applied to the crystal between electrodes separated by distance l. Notice that $\boldsymbol{E} = E\boldsymbol{i}$.

Even though the space-charge field E can be obtained in principle from Eqs. (4)–(7), this task is considerably involved. However, we can conveniently derive E by taking a similar way to that of Ref. [14]. In typical PR materials N_D^+, N_D, $N_A \gg n$ [5,14]. In this case, Eq. (6) yields

$$N_D^+ = N_A\left(1 + L_D \frac{\partial}{\partial x}\frac{E}{E_t}\right), \tag{8}$$

where $E_t = k_B T/eL_D = eN_A L_D/\epsilon_0\epsilon_r$, $L_D = (\epsilon_0 \epsilon_r k_B T/e^2 N_A)^{1/2}$ is Debye length. Substitution of Eq. (8) into Eq. (4) yields

$$n = \frac{\hat{s}I + \beta_T}{\gamma f}\left(1 + L_D\frac{\partial}{\partial x}\frac{E}{E_t}\right)^{-1}\left(1 - fL_D\frac{\partial}{\partial x}\frac{E}{E_t}\right), \tag{9}$$

where $f = N_A/(N_D - N_A)$. When $x \to \pm\infty$, $E(x \to \pm\infty, z) = E_0$ (constant), $\partial E/\partial x = 0$ and $N_D^+ = N_A$. Thus, Eqs. (5) and (9) yield the following result

$$J_\infty = e\hat{\mu} n_\infty E_0 + \kappa \hat{s}(N_D - N_A) I_\infty, \tag{10}$$

where $n_\infty = n(x \to \pm\infty) = (\hat{s}I_\infty + \beta_T)/\gamma f$ and $I_\infty = I(x \to \pm\infty)$. Equation (5) implies that J is constant everywhere and therefore $J = J_\infty$. In this case, one can get the space-charge field

$$\begin{aligned} E = {} & \left(E_0 \frac{I_\infty + I_d}{I + I_d} - E_p \frac{I - I_\infty}{I + I_d} + E_p \frac{I}{I + I_d} f L_D \frac{\partial}{\partial x}\frac{E}{E_t}\right) \\ & \times \left(1 + L_D \frac{\partial}{\partial x}\frac{E}{E_t}\right)\left(1 - fL_D\frac{\partial}{\partial x}\frac{E}{E_t}\right)^{-1} \\ & - \frac{k_B T}{e}\left\{\frac{\partial}{\partial x}\ln(I + I_d) - \left[\left(1 + L_D\frac{\partial}{\partial x}\frac{E}{E_t}\right)^{-1}\right.\right. \\ & \left.\left. + f\left(1 - fL_D\frac{\partial}{\partial x}\frac{E}{E_t}\right)^{-1}\right] L_D \frac{\partial^2}{\partial x^2}\frac{E}{E_t}\right\}, \end{aligned} \tag{11}$$

where $E_p = \kappa\gamma N_A/e\hat{\mu}$ is the PV field constant, and $I_d = \beta_T/\hat{s}$. If the intensity $I(x,z)$ varies smoothly with respect to x, the diffusion effects in typical PR media may be neglected relative to the PV effects in Eq. (11) [5,14], and the dimensionless term $L_D \partial E/\partial x$ is expected to be much less than unity [5,14]. Thus, by taking a similar way to that of Ref. [4], from Eqs. (7) and (11) we obtain

$$E=-(\epsilon\eta+E_p\hat{\sigma}\eta)\frac{I_\infty+I_d}{I+I_d}+E_p\frac{I_\infty-I}{I+I_d}, \qquad (12)$$

where $\eta=1/\int_{-l/2}^{l/2}(I_\infty+I_d)/(I+I_d)\,dx$, and $\hat{\sigma}=\int_{-l/2}^{l/2}(I_\infty-I)/(I+I_d)\,dx$. The total power density of the two optical beams can be obtained by summing the two Poynting fluxes, i.e., $I=(n_e/2\eta_0)(|\phi|^2+|\psi|^2)$, where $\eta_0=(\mu_0/\epsilon_0)^{1/2}$. Moreover, for simplicity, let us adopt the following dimensionless variables and coordinates, i.e., let $\phi=(2\eta_0 I_d/n_e)^{1/2}U$, $\psi=(2\eta_0 I_d/n_e)^{1/2}V$, $\xi=z/(kx_0^2)$, and $s=x/x_0$. x_0 is an arbitrary spatial width, and the power densities of the optical and beams have been scaled with respect to the dark irradiance I_d. By employing these latter transformations and by substituting Eq. (12) in Eqs. (2) and (3), we find that the normalized envelopes U and V obey the following dynamical evolution equation:

$$iU_\xi+\frac{1}{2}U_{ss}+(\alpha+\beta)(\rho+1)\frac{U}{1+|U|^2+|V|^2}-\delta\frac{[\rho-(|U|^2+|V|^2)]U}{1+|U|^2+|V|^2}=0, \qquad (13)$$

$$iV_\xi+\frac{1}{2}V_{ss}+(\alpha+\beta)(\rho+1)\frac{V}{1+|U|^2+|V|^2}-\delta\frac{[\rho-(|U|^2+|V|^2)]V}{1+|U|^2+|V|^2}=0, \qquad (14)$$

where $\rho=I_\infty/I_d$, $\beta=(k_0x_0)^2(n_e^4 r_{33}\eta/2)\epsilon$, $\alpha=(k_0x_0)^2(n_e^4 r_{33}\hat{\sigma}\eta/2)E_P$, and $\delta=(k_0x_0)^2(n_e^4 r_{33}/2)E_P$. To simplify the analysis, we have neglected any loss effects in Eqs. (13) and (14).

We begin our analysis by considering first bright–bright soliton pairs. In this case, where bright optical beams are involved in both components, the intensity is expected to vanish at infinity ($s\to\pm\infty$) and thus $I_\infty=\rho=0$. From Eqs. (13) and (14), we find that

$$iU_\xi+\frac{1}{2}U_{ss}+(\alpha+\beta)\frac{U}{1+|U|^2+|V|^2}+\delta\frac{(|U|^2+|V|^2)U}{1+|U|^2+|V|^2}=0, \qquad (15)$$

$$iV_\xi+\frac{1}{2}V_{ss}+(\alpha+\beta)\frac{V}{1+|U|^2+|V|^2}+\delta\frac{(|U|^2+|V|^2)V}{1+|U|^2+|V|^2}=0. \qquad (16)$$

The solutions of Eqs. (15) and (16) can be readily obtained by expressing the normalized envelopes U and V in the following way: $U=r^{1/2}y(s)\cos\theta\exp(i\mu\xi)$ and $V=r^{1/2}y(s)\sin\theta\exp(i\mu\xi)$, where μ represents a nonlinear shift of the propagation constant, θ is an arbitrary projection angle, and $y(s)$ is a normalized real function bounded between $0\leqslant y(s)\leqslant 1$. Substitution of these forms of U and V into Eqs. (15) and (16) yields

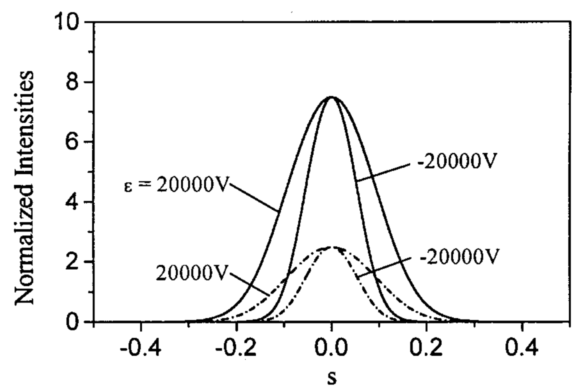

FIG. 1. Soliton components, $|U|^2$ (solid curve) and $|V|^2$ (dashed-dotted curve), for bright–bright pairs when $r=10$, $\theta=\pi/6$, and $\epsilon=\pm 20\,000$ V are shown.

$$y''-2\mu y+2(\alpha+\beta)\frac{y}{1+ry^2}+2\delta\frac{ry^3}{1+ry^2}=0, \qquad (17)$$

with $y(0)=0$, $y'(0)=0$, and $y(s\to\pm\infty)=0$, where $y''=d^2y/ds^2$. By integrating Eq. (17) and by employing the y-boundary conditions, we obtain

$$\mu=-\frac{\delta-\beta-\alpha}{r}\ln(1+r)+\delta, \qquad (18)$$

$$(y')^2=\frac{2(\delta-\beta-\alpha)}{r}[\ln(1+ry^2)-y^2\ln(1+r)]. \qquad (19)$$

Further integration of Eq. (19) leads to

$$[2(\delta-\beta-\alpha)]^{1/2}s=\pm\int_y^1\frac{r^{1/2}\,d\hat{y}}{[\ln(1+r\hat{y}^2)-\hat{y}^2\ln(1+r)]^{1/2}}, \qquad (20)$$

from which the bright envelope $y(s)$ can be determined. It is proved that the quantity in the square bracket of Eq. (19) is always for all values of $(y')^2$ between $0\leqslant y(s)\leqslant 1$. Therefore, bright solitons will be possible only when $(\delta-\beta-\alpha)>0$ (so as $(y')^2>0$). In this case, the soliton pair components can be considered as the θ projections of the fundamental bright soliton envelope. To illustrate our results, we consider the following examples: let $\lambda_0=0.5\,\mu$m, $l=1$ cm, $x_0=40\,\mu$m, and $\epsilon=\pm 20\,000$ V. The $LiNbO_3$ parameters are taken here to $n_e=2.2$, $r_{33}=30\times 10^{-12}$ m/V, and $E_p=40$ kV/cm. Figure 1 depicts the normalized intensity profiles of these soliton pairs when $r=10$, $\theta=\pi/6$, and $\epsilon=\pm 20\,000$ V.

The case of dark–dark soliton pairs can also be analyzed in a similar fashion. These dark beams exhibit an antisymmetric field profile (with respect to x) and, moreover, they are embedded in a constant intensity background I_∞, that is, I_∞ and ρ are finite quantities. Therefore, from Eqs. (13) and (14) dark-type pair envelopes U and V should evolve according to

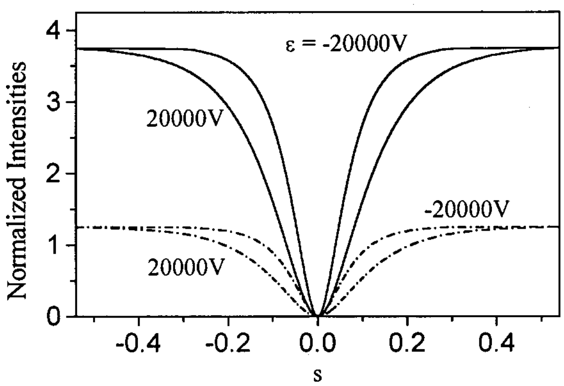

FIG. 2. Soliton components, $|U|^2$ (solid curve) and $|V|^2$ (dashed-dotted curve), for dark–dark pairs when $\rho=5$, $\theta=\pi/6$, and $\epsilon=\pm 20\,000$ V are shown.

$$iU_\xi+\frac{1}{2}U_{ss}+\frac{(\alpha+\beta)(\rho+1)U}{1+|U|^2+|V|^2}-\frac{\delta[\rho-(|U|^2+|V|^2)]U}{1+|U|^2+|V|^2}=0, \tag{21}$$

$$iV_\xi+\frac{1}{2}V_{ss}+\frac{(\alpha+\beta)(\rho+1)V}{1+|U|^2+|V|^2}-\frac{\delta[\rho-(|U|^2+|V|^2)]V}{1+|U|^2+|V|^2}=0. \tag{22}$$

To obtain dark–dark soliton pair solutions of Eqs. (21) and (22), let us express the envelopes U and V in the following way: $U=\rho^{1/2}y(s)\cos\theta\exp(i\mu\xi)$ and $V=\rho^{1/2}y(s)\sin\theta\exp(i\mu\xi)$, where $|y(s)|\leqslant 1$. Substitution of these forms of U and V into Eqs. (21) and (22) yields

$$y''-2\mu y+2(\alpha+\beta)(\rho+1)\frac{y}{1+\rho y^2}-2\delta\rho\frac{(1-y^2)y}{1+\rho y^2}=0, \tag{23}$$

with $y(s\to\pm\infty)=\pm 1$, $y(0)=0$, and all the derivatives of $y(s)$ vanish at infinity. Using the boundary conditions of $y(s)$ at infinity and substituting $s\to\infty$ into Eq. (23) leads to

$$\mu=\beta+\alpha. \tag{24}$$

We integrate Eq. (23) leads to

$$(\dot{y})^2=-2(\delta-\beta-\alpha)\left[(y^2-1)-\frac{\rho+1}{\rho}\ln\left(\frac{1+\rho y^2}{1+\rho}\right)\right]. \tag{25}$$

Further integration of Eq. (25) leads to

$$[-2(\delta-\beta-\alpha)]^{1/2}s=\pm\int_y^0\frac{d\hat{y}}{\left[(\hat{y}^2-1)-\frac{\rho+1}{\rho}\ln\left(\frac{1+\rho\hat{y}^2}{1+\rho}\right)\right]^{1/2}}, \tag{26}$$

from which the dark envelope $y(s)$ can be obtained. It can be readily shown that the quantity in the square bracket of Eq. (25) remains positive for all values of $y^2\leqslant 1$. Therefore, dark solitons will be possible only when $(\delta-\beta-\alpha)$ is negative [so that $(y')^2>0$]. The pair components can then be simply obtained through a θ projection. A particular case of $\rho=5$ and $\theta=\pi/6$ is shown in Fig. 2. When $\lambda_0=0.5\ \mu$m, $l=1$ cm, $x_0=40\ \mu$m, and $\epsilon=\pm 20\,000$ V. The $LiNbO_3$ parameters are taken to be the same as those considered in the previous examples.

To find the bright–dark soliton pair solutions of Eqs. (13) and (14), the normalized envelopes U and V are expressed in the following way, $U=r^{1/2}f(s)\exp(i\mu\xi)$ and $V=\rho^{1/2}g(s)\exp(i\nu\xi)$, where $f(s)$ corresponds to a bright beam envelope and $g(s)$ to a dark one. Hence, $f(0)=1$, $f'(0)=0$, $f(s\to\pm\infty)=0$, $g(0)=0$, $g(s\to\pm\infty)=\pm 1$, and moreover, all the derivatives of $f(s)$ and $g(s)$ are assumed to vanish at infinity. The positive variables r and ρ represent the ratios of their maximum power density with respect to the dark irradiance I_d. Direct substitution of these forms of U and V in Eqs. (13) and (14) yields the following results:

$$f''=2\left[\mu-\frac{(\alpha+\beta)(\rho+1)}{1+rf^2+\rho g^2}+\frac{\delta(\rho-rf^2-\rho g^2)}{1+rf^2+\rho g^2}\right]f, \tag{27}$$

$$g''=2\left[\nu-\frac{(\alpha+\beta)(\rho+1)}{1+rf^2+\rho g^2}+\frac{\delta(\rho-rf^2-\rho g^2)}{1+rf^2+\rho g^2}\right]g, \tag{28}$$

where $f''=d^2f/ds^2$, etc. We now look for particular solutions that also satisfy the condition $f^2+g^2=1$. In this case, Eqs. (27) and (28) yield the following forms

$$f''=2\left[\mu-(\alpha+\beta)\frac{1}{1+\sigma f^2}-\delta\frac{\sigma f^2}{1+\sigma f^2}\right]f, \tag{29}$$

$$g''=2\left[\nu-(\alpha+\beta)\frac{1}{1+\sigma(1-g^2)}-\delta\frac{\sigma(1-g^2)}{1+\sigma(1-g^2)}\right]g, \tag{30}$$

where $\sigma=(r-\rho)/(1+\rho)$. Integration of Eqs. (29) and (30) leads to

$$\mu=-\frac{\delta-\beta-\alpha}{r}\ln(1+\sigma)+\delta, \tag{31}$$

$$(f')^2=\frac{2(\delta-\beta-\alpha)}{\sigma}[\ln(1+\sigma f^2)-f^2\ln(1+\sigma)], \tag{32}$$

$$\nu=\beta+\alpha, \tag{33}$$

$$(g')^2=2(\delta-\beta-\alpha)\left[(1-g^2)+\ln\left(\frac{1+\sigma y^2}{1+\sigma}\right)\right]. \tag{34}$$

The quantity in the square bracket of Eqs. (32) and (34) is always positive for ally values of $f^2+g^2=1$. Therefore, the solutions of Eq. (32) are possible when $[(\delta-\beta-\alpha)/\sigma]>0$ [so as $(f')^2>0$], and the solutions of Eq. (34) are possible when $(\delta-\beta-\alpha)>0$. On the other hand, when the peak intensities of the two beams are approximately equal, i.e., $|\sigma|\leqslant 1$, one can get an approximate analytic solution for the bright–dark soliton pair wave forms. In this case, μ is approximately given by $\mu\cong\delta-(\delta-\beta-\alpha)(1-\sigma/2)$. Thus, Eqs. (32) and (34) can be simplified to

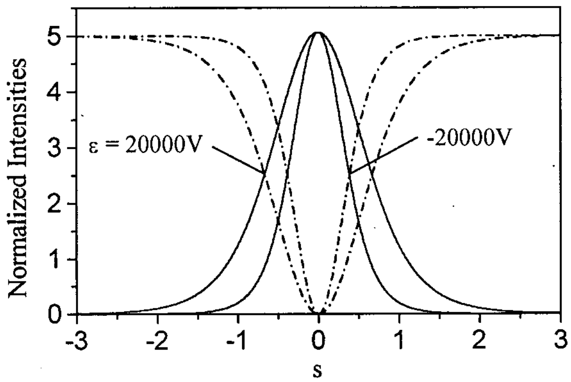

FIG. 3. Soliton components, $|U|^2$ (solid curve) and $|V|^2$ (dashed-dotted curve), for bright–dark pairs when $\rho=5$, $\sigma=0.01$, and $\epsilon=\pm 20\,000$ V are shown.

$$f''=(\delta-\beta-\alpha)\sigma f-2(\delta-\beta-\alpha)\sigma f^3, \tag{35}$$

$$f''=-2(\delta-\beta-\alpha)\sigma g+2(\delta-\beta-\alpha)\sigma g^3. \tag{36}$$

Equations (35) and (36) can be integrated once and lead to

$$f=\mathrm{sech}\{[(\delta-\beta-\alpha)\sigma]^{1/2}s\}, \tag{37}$$

$$g=\tanh\{[(\delta-\beta-\alpha)\sigma]^{1/2}s\}. \tag{38}$$

Note that these solutions are also consistent with our previous condition $f^2+g^2=1$. The approximate soliton pair solutions of Eqs. (13) and (14) for $|\sigma|\ll 1$ are given by

$$U=r^{1/2}\,\mathrm{sech}\{[(\delta-\beta-\alpha)\sigma]^{1/2}s\}\times\exp\{i[(\beta+\alpha)+(\delta-\beta-\alpha)\sigma/2]\xi\}, \tag{39}$$

$$V=\rho^{1/2}\tanh\{[(\delta-\beta-\alpha)\sigma]^{1/2}s\}\exp[i(\beta+\alpha)\xi]. \tag{40}$$

These equations clearly show that these solutions are possible only when $(\delta-\beta-\alpha)\sigma>0$. The soliton pairs obtained for $\rho=5$ in the $LiNbO_3$ are shown in Fig. 3. When $\sigma=0.01$, $\lambda_0=0.5$ μm, $l=1$ cm, $x_0=40$ μm, and $\epsilon=\pm 20\,000$ V.

Now let us consider incoherently coupled $2N$-component spatial solitons in biased photorefractive-photovoltaic materials. For simplicity, we assume that $2N$ self-trapped mutually incoherent optical beams are made up of $\Sigma_{j=1}^{N}E_j$ and $\Sigma_{m=1}^{N}E_m$. A similar way is taken to that of studying previously incoherently coupled two-component spatial solitons. By expressing $\Sigma_{j=1}^{N}\boldsymbol{E}_j$ and $\Sigma_{m=1}^{N}\boldsymbol{E}_m$ in terms of a slowly varying envelopes $\Sigma_{j=1}^{N}\phi_j$ and $\Sigma_{m=1}^{N}\psi_m$, i.e., $\Sigma_{j=1}^{N}\boldsymbol{E}_j=\Sigma_{j=1}^{N}\boldsymbol{i}\phi_j(x,z)\exp(ikz)$, and $\Sigma_{m=1}^{N}\boldsymbol{E}_m=\Sigma_{m=1}^{N}\boldsymbol{i}\psi_m(x,z)\exp(ikz)$, we find that the Helmholtz equation leads to the following evolution equations:

$$i\frac{\partial\phi_j}{\partial z}+\frac{1}{2k}\frac{\partial^2\phi_j}{\partial x^2}-\frac{k_0(n_e^3r_{33}E)}{2}\phi_j=0, \tag{41}$$

$$i\frac{\partial\psi_m}{\partial z}+\frac{1}{2k}\frac{\partial^2\psi_m}{\partial x^2}-\frac{k_0(n_e^3r_{33}E)}{2}\psi_m=0, \tag{42}$$

where $\phi_j(x,z)$ and $\psi_m(x,z)$ denote the jth component and the mth component envelope of the optical beams, respectively. For the $2N$ mutually incoherent optical beams, the total optical power density is $I=(n_e/2\eta_0)(\Sigma_{j=1}^{N}|\phi_j|^2+\Sigma_{m=1}^{N}|\psi_m|^2)$. By employing $\phi_j=(2\eta_0I_d/n_e)^{1/2}U_j$, $\psi_m=(2\eta_0I_d/n_e)^{1/2}V_m$, $\xi=z/(kx_0^2)$, and $s=x/x_0$, and by substituting Eq. (12) into Eqs. (41) and (42), we find that

$$i\frac{\partial U_j}{\partial\xi}+\frac{1}{2}\frac{\partial^2U_j}{\partial s^2}+(\alpha+\beta)(\rho+1)\times\frac{U_j}{1+\sum_{j=1}^{N}|U_j|^2+\sum_{m=1}^{N}|V_m|^2}-\delta\frac{\left[\rho-\left(\sum_{j=1}^{N}|U_j|^2+\sum_{m=1}^{N}|V_m|^2\right)\right]U_j}{1+\sum_{j=1}^{N}|U_j|^2+\sum_{m=1}^{N}|V_m|^2}=0, \tag{43}$$

$$i\frac{\partial V_m}{\partial\xi}+\frac{1}{2}\frac{\partial^2V_m}{\partial s^2}+(\alpha+\beta)(\rho+1)\times\frac{V_m}{1+\sum_{j=1}^{N}|U_j|^2+\sum_{m=1}^{N}|V_m|^2}-\delta\frac{\left[\rho-\left(\sum_{j=1}^{N}|U_j|^2+\sum_{m=1}^{N}|V_m|^2\right)\right]V_m}{1+\sum_{j=1}^{N}|U_j|^2+\sum_{m=1}^{N}|V_m|^2}=0. \tag{44}$$

In what follows, we will discuss the possible soliton solutions of Eqs. (43) and (44).

$2N$-component bright solitons.—The boundary condition for the bright soliton is $I_\infty=0$, i.e., $\rho=0$. Soliton solutions can be obtained by expressing the normalized envelopes $\Sigma_{j=1}^{N}U_j$ and $\Sigma_{m=1}^{N}V_m$ in the following way:

$$\sum_{j=1}^{N}U_j=\sum_{j=1}^{N}\frac{1}{\sqrt{N}}r^{1/2}y(s)\cos(j\theta)\exp(i\mu\xi), \tag{45}$$

$$\sum_{m=1}^{N}V_m=\sum_{m=1}^{N}\frac{1}{\sqrt{N}}r^{1/2}y(s)\sin(m\theta)\exp(i\mu\xi). \tag{46}$$

Notice that the set (N,θ) has to be judiciously selected so that the optical beams $\Sigma_{j=1}^{N}\mathbf{E}_j$ and $\Sigma_{m=1}^{N}\mathbf{E}_m$ include $2N$ components of different beam intensity. By substituting these forms of $\Sigma_{j=1}^{N}U_j$ and $\Sigma_{m=1}^{N}V_m$ into Eqs. (43) and (44), we obtain

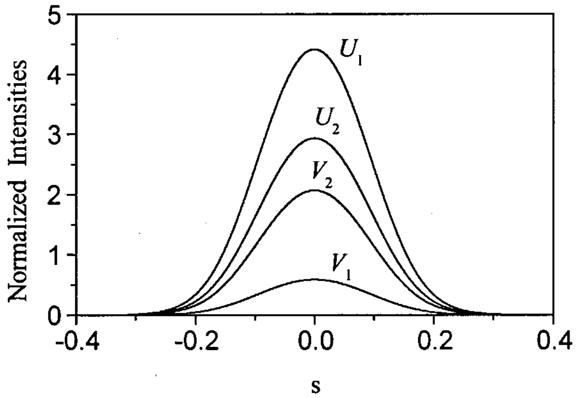

FIG. 4. Soliton components, $\Sigma_{j=1}^{N}U_j$ and $\Sigma_{m=1}^{N}V_m$, for incoherently coupled multicomponent bright solitons when $\theta=20°$, $r=10$, $N=2$, $\lambda_0=0.5\,\mu$m, $l=1$ cm, $x_0=40\,\mu$m, and $\epsilon=20\,000$ V are shown.

$$y''-2\mu y+2(\alpha+\beta)\frac{y}{1+ry^2}+2\delta\frac{ry^3}{1+ry^2}=0, \tag{47}$$

which is known to allow bright solitons when $(\delta-\beta-\alpha)>0$ and $\mu=-\delta-\beta-\alpha/r\ln(1+r)+\delta$ [Eq. (47) has been discussed in great detail in the previous bright–bright soliton pairs]. We can obtain the multicomponent composite bright soliton components through a θ projection. Figure 4 depicts the normalized intensity profiles of incoherently coupled multicomponent bright solitons in the $LiNbO_3$ when $\theta=20°$, $N=2$, $\lambda_0=0.5$ μm, $l=1$ cm, $x_0=40$ μm, and $\epsilon=20\,000$ V.

$2N$*-component dark solitons*.—One requires I_∞ and ρ are finite quantities. The envelopes $\Sigma_{j=1}^{N}U_j$ and $\Sigma_{m=1}^{N}V_m$ are expressed again as

$$\sum_{j=1}^{N}U_j=\sum_{j=1}^{N}\frac{1}{\sqrt{N}}\rho^{1/2}y(s)\cos(j\theta)\exp(i\mu\xi), \tag{48}$$

$$\sum_{m=1}^{N}V_m=\sum_{m=1}^{N}\frac{1}{\sqrt{N}}\rho^{1/2}y(s)\sin(m\theta)\exp(i\mu\xi). \tag{49}$$

Therefore, from Eqs. (43), (44), (48), and (49), $2N$-component dark solitons should satisfy

$$y''-2\mu y+2(\alpha+\beta)(\rho+1)\frac{y}{1+\rho y^2}-2\delta\rho\frac{(1-y^2)y}{1+\rho y^2}=0, \tag{50}$$

which is known to be possible when $(\delta-\beta-\alpha)$ is negative and $\mu=\beta+\alpha$ [Eq. (50) has been discussed in the previous dark–dark soliton pairs]. The multicomponent composite dark soliton components can be simply obtained through a θ projection. Figure 5 depicts the normalized intensity profiles of the incoherently coupled multicomponent dark solitons in the $LiNbO_3$ when $\theta=20°$, $N=2$, $\lambda_0=0.5\,\mu$m, $l=1$ cm, $x_0=40\,\mu$m, and $\epsilon=20\,000$ V.

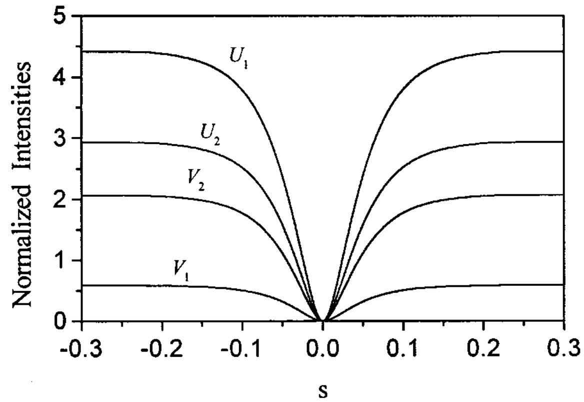

FIG. 5. Soliton components, $\Sigma_{j=1}^{N}U_j$ and $\Sigma_{m=1}^{N}V_m$, for incoherently coupled multicomponent dark solitons when $\theta=20°$, $\rho=5$, $N=2$, $\lambda_0=0.5$ μm, $l=1$ cm, $x_0=40$ μm, and $\epsilon=20\,000$ V are shown.

N-component bright-dark solitons.—To find a solution of this sort, the normalized envelopes $\Sigma_{j=1}^{N}U_j$ and $\Sigma_{m=1}^{N}V_m$ are expressed in the following way:

$$\begin{aligned}\sum_{j=1}^{N}U_j=&\sum_{j=1}^{N/2}\frac{1}{\sqrt{N/2}}r^{1/2}f(s)\cos(j\theta)\exp(i\mu\xi)\\&+\sum_{j=N/2+1}^{N}\frac{1}{\sqrt{N/2}}r^{1/2}f(s)\\&\times\sin\{[(N+1)-j]\theta\}\exp(i\mu\xi),\end{aligned} \tag{51}$$

$$\begin{aligned}\sum_{m=1}^{N}V_m=&\sum_{m=1}^{N/2}\frac{1}{\sqrt{N/2}}\rho^{1/2}g(s)\cos(m\theta)\exp(i\nu\xi)\\&+\sum_{m=N/2+1}^{N}\frac{1}{\sqrt{N/2}}\rho^{1/2}g(s)\\&\times\sin\{[(N+1)-m]\theta\}\exp(i\nu\xi),\end{aligned} \tag{52}$$

where N is restricted to even numbers. Substituting Eqs. (51) and (52) into Eqs. (43) and (44) leads to

$$f''=2\left[\mu-\frac{(\alpha+\beta)(\rho+1)}{1+rf^2+\rho g^2}+\frac{\delta(\rho-rf^2-\rho g^2)}{1+rf^2+\rho g^2}\right]f, \tag{53}$$

$$g''=2\left[\nu-\frac{(\alpha+\beta)(\rho+1)}{1+rf^2+\rho g^2}+\frac{\delta(\rho-rf^2-\rho g^2)}{1+rf^2+\rho g^2}\right]g, \tag{54}$$

which have been discussed in the previous bright–dark soliton pairs, and are given by $f=\text{sech}\{[(\delta-\beta-\alpha)\sigma]^{1/2}s\}$ and $g=\tanh\{[(\delta-\beta-\alpha)\sigma]^{1/2}s\}$. The incoherently coupled multicomponent bright–dark solitons obtained for $\rho=5$ in the $LiNbO_3$ are shown in Fig. 6. when $\theta=20°$, $N=4$, $\sigma=0.01$, $\lambda_0=0.5$ μm, $l=1$ cm, $x_0=40$ μm, and $\epsilon=20\,000$ V.

The stability properties of these soliton pairs and multicomponent spatial solitons will now be discussed. In particular, their stability is investigated here using the modulation instability theory. For incoherent beams in noninstantaneous

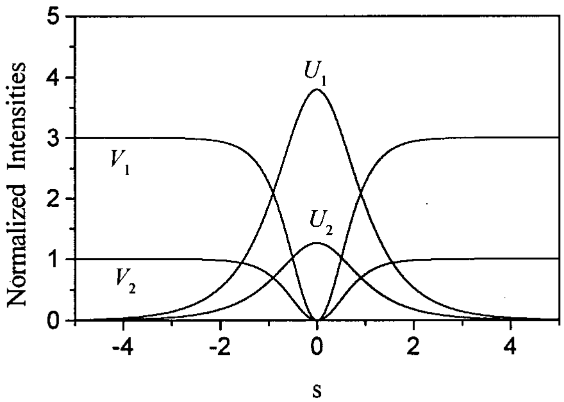

FIG. 6. Soliton components, $\Sigma_{j=1}^{N} U_j$ and $\Sigma_{m=1}^{N} V_m$, for incoherently coupled multicomponent bright–dark solitons when $\theta = 20°$, $\rho = 5$, $N = 4$, $\sigma = 0.01$, $\lambda_0 = 0.5\ \mu$m, $l = 1$ cm, $x_0 = 40\ \mu$m, and $\epsilon = 20\,000$ V are shown.

nonlinear media, modulation instability exists only when $\hat{\kappa} I_0 / n_e > \hat{\theta}_0^2$, where $\hat{\kappa} = d\,\delta n(I)/dI$ evaluated at I_0 is the marginal nonlinear index, $\delta n(I)$ is the tiny nonlinear modification to the refractive index, $\hat{\theta}_0$ is the angular power spectrum (spatial degree of coherence), whereas when $\hat{\kappa} I_0 / n_e < \hat{\theta}_0^2$, the modification instability is entirely eliminated [30]. In photorefractives, $\delta n(I) = -\frac{1}{2} n_e^3 r_{33} E$. Thus, Eq. (12) yields the following results:

$$\hat{\kappa} I_0 / n_e = G r_{33}(E_p - E_p \hat{\sigma} \eta - \epsilon \eta), \tag{55}$$

where $G = n_e^2 I_0(\rho+1)/2(I_d + I_0) > 0$. When $G r_{33}(E_p - E_p \hat{\sigma} \eta - \epsilon \eta) < \hat{\theta}^2$, these soliton pairs and multicomponent spatial solitons are stable because incoherent modulation instability is entirely eliminated. On the other hand, when $G|r_{33}(E_p - E_p \hat{\sigma} \eta - \epsilon \eta)| > \hat{\theta}^2$, bright–dark soliton pairs and N-component bright–dark solitons are stable in the range of $r_{33}(E_p - E_p \hat{\sigma} \eta - \epsilon \eta) < 0$; however, they are unstable in the range of $r_{33}(E_p - E_p \hat{\sigma} \eta - \epsilon \eta) > 0$ because incoherent modulation instability exists in the range of $G r_{33}(E_p - E_p \hat{\sigma} \eta - \epsilon \eta) < \hat{\theta}^2$. In order to explain that our analyses are correct, let $E_p = 0$. In this case, $\hat{\kappa} I_0 / n_e = G r_{33} E_0$. Notice that $E_0 = -\epsilon \eta$. According to the modulation instability theory, when $G|r_{33} E_0| > \hat{\theta}^2$, for $r_{33} E_0 < 0$ (i.e., $\hat{\beta} = (k_0 x_0)^2 (n_e^4 r_{33} \eta/2) E_0 < 0$), bright–dark soliton pairs for screening solitons are stable; however, for $r_{33} E_0 > 0$, they are unstable. This result is the same for result of numerical techniques for bright–dark soliton pairs of screening solitons [20].

Next, we discuss the relation between the space-charge field in biased photorefractive-photovoltaic crystals and the space-charge field of both screening and PV solitons. When the bulk PV effect is neglectable, i.e., $E_p = 0$, the physical system of SP solitons becomes the physical system of the previously studied screening solitons. In this case, Eq. (12) reads

$$E = E_0 \frac{I_\infty + I_d}{I + I_d}. \tag{56}$$

Equation (56) has the same dimensionless parameters and form as Eq. (12) of Ref. [5], in which the screening solitons are discussed for the biased photorefractive-nonphotovoltaic crystals. When the external bias field is absent, $N_A / N_D \ll 1$ [13] and Eqs. (5) and (9) yield

$$\hat{J} = \frac{I_\infty - \sigma \eta (I_\infty + I_d)}{I_d}, \tag{57}$$

where $\hat{J} = J/(\hat{s} I_d N_D \kappa)$ [13]. Substituting Eq. (57), $\epsilon = 0$ and $I = u^2(\hat{\xi}) I_d$ into Eq. (12) yields

$$\hat{E} = \frac{\hat{J} - u^2}{1 + u^2}, \tag{58}$$

Equation (58) has the same dimensionless parameters and form as Eq. (13) for the open- and closed-circuit conditions in Ref. [13], in which PV solitons are discussed in photorefractive-photovoltaic crystals without the external bias field. To illustrate further our result for the open circuit, substituting $\hat{J} = 0$, $\hat{E} = E/E_p$, and $I = u^2 I_d$ into Eq. (58) yields

$$E = -E_p \frac{I/I_d}{1 + I/I_d}. \tag{59}$$

Equation (59) has the same dimensionless parameters and form as Eq. (6) for the open circuit in Ref. [10], in which PV solitons are discussed in photorefractive-photovoltaic crystals for the open circuit.

Finally, we discuss the properties of the incoherently coupled soliton pairs and the multicomponent spatial solitons in biased photorefractive-photovoltaic crystals. First of all, soliton pairs for screening and PV solitons can be simply obtained from the incoherently coupled soliton pairs in biased photorefractive-photovoltaic crystals under appropriate conditions. When the bulk photovoltaic effect is neglectable, i.e., $\delta = \alpha = 0$, substituting $\beta = -(k_0 x_0)^2 (n_e^4 r_{33} \eta/2) E_0 = -\hat{\beta}$ into Eqs. (13), (14), (17), (23), (27), (28), (39), and (40) yields

$$i U_\xi + \frac{1}{2} U_{ss} - \hat{\beta}(\rho+1) \frac{U}{1 + |U|^2 + |V|^2} = 0, \tag{60}$$

$$i V_\xi + \frac{1}{2} V_{ss} - \hat{\beta}(\rho+1) \frac{V}{1 + |U|^2 + |V|^2} = 0, \tag{61}$$

$$y'' - 2\mu y - 2\hat{\beta} \frac{y}{1 + r y^2} = 0, \tag{62}$$

$$y'' - 2\mu y - 2\hat{\beta}(\rho+1) \frac{y}{1 + \rho y^2} = 0, \tag{63}$$

$$f''=2\left[\mu+\frac{\hat{\beta}(\rho+1)}{1+rf^2+\rho g^2}\right]f, \tag{64}$$

$$g''=2\left[\nu+\frac{\hat{\beta}(\rho+1)}{1+rf^2+\rho g^2}\right]g, \tag{65}$$

$$U=r^{1/2}\,\mathrm{sech}\{[\hat{\beta}\sigma]^{1/2}s\}\exp[-i\hat{\beta}(1-\sigma/2)\xi], \tag{66}$$

$$V=\rho^{1/2}\tanh\{[\hat{\beta}\sigma]^{1/2}s\}\exp[-i\hat{\beta}\xi]. \tag{67}$$

Equations (60)–(67) have the same dimensionless parameters and form as Eqs. (4)–(11) in Ref. [20], in which incoherently coupled soliton pairs are discussed for screening solitons. When the external bias field is absent, i.e., $\beta=0$, Eqs. (13), (14), (17), (23), (27), (28), (39), and (40) yield

$$iU_\xi+\frac{1}{2}U_{ss}+\alpha(\rho+1)\frac{U}{1+|U|^2+|V|^2}-\delta\frac{[\rho-(|U|^2+|V|^2)]U}{1+|U|^2+|V|^2}=0, \tag{68}$$

$$iV_\xi+\frac{1}{2}V_{ss}+\alpha(\rho+1)\frac{V}{1+|U|^2+|V|^2}-\delta\frac{[\rho-(|U|^2+|V|^2)]V}{1+|U|^2+|V|^2}=0, \tag{69}$$

$$y''-2\mu y+2\alpha\frac{y}{1+ry^2}+2\delta\frac{ry^3}{1+ry^2}=0, \tag{70}$$

$$y''-2\mu y+2\alpha(\rho+1)\frac{y}{1+\rho y^2}-2\delta\rho\frac{(1-y^2)y}{1+\rho y^2}=0, \tag{71}$$

$$f''=2\left[\mu-\frac{\alpha(\rho+1)}{1+rf^2+\rho g^2}+\frac{\delta(\rho-rf^2-\rho g^2)}{1+rf^2+\rho g^2}\right]f, \tag{72}$$

$$g''=2\left[\nu-\frac{\alpha(\rho+1)}{1+rf^2+\rho g^2}+\frac{\delta(\rho-rf^2-\rho g^2)}{1+rf^2+\rho g^2}\right]g, \tag{73}$$

$$U=r^{1/2}\,\mathrm{sech}\{[(\delta-\alpha)\sigma]^{1/2}s\}\exp\{i[\alpha+(\delta-\alpha)\delta/2]\xi\}, \tag{74}$$

$$V=\rho^{1/2}\tanh\{[(\delta-\alpha)\sigma]^{1/2}s\}\exp[i\alpha\xi]. \tag{75}$$

Equations (68)–(75) predict incoherently coupled soliton pairs for PV solitons. Moreover, under appropriate conditions incoherently coupled multicomponent spatial solitons in biased photorefractive-photovoltaic crystals predict incoherently coupled multicomponent spatial solitons for screening and PV solitons. When the bulk photovoltaic effect is neglectable, i.e., $\delta=\alpha=0$, incoherently coupled multicomponent bright solitons for screening solitons can be determined from Eqs. (45), (46), and (20), incoherently coupled multicomponent dark solitons for screening solitons can be determined from Eqs. (45), (46), and (26), and incoherently coupled multicomponent bright and dark solitons for screening solitons can be determined from Eqs. (45), (46), (37), and (38). When the external bias field is absent, i.e., $\beta=0$, incoherently coupled multicomponent bright solitons for PV solitons can be obtained from Eqs. (45), (46), and (20), incoherently coupled multicomponent dark solitons for PV solitons can be obtained from Eqs. (45), (46), and (26), and incoherently coupled multicomponent bright and dark solitons for PV solitons can be obtained from Eqs. (45), (46), (37), and (38).

In conclusion, we have shown that a kind of the incoherently coupled soliton pairs and multicomponent spatial solitons are possible in biased photorefractive-photovoltaic crystals under steady-state conditions, which result from both the bulk PV effect and the spatially nonuniform screening of the external bias field. These soliton states can be obtained provided that their carrier beams share the same polarization and wavelength, and are mutually incoherent. If the bulk PV effect is neglectable, these soliton pairs are the previously studied soliton pairs for screening solitons, these multicomponent spatial solitons predict incoherently coupled multicomponent spatial solitons for screening solitons, and their space-charge field is the space-charge field of screening solitons. If the external field is absent, these soliton pairs and multicomponent spatial solitons predict incoherently coupled soliton pairs and multicomponent spatial solitons for PV solitons, and their space-charge field is the space-charge field of PV solitons. Their stability properties were also investigated using modulation instability theory.

This work was supported by the Chinese National Nature Sciences Foundation (Grant No. 69978019) and the State Key Laboratory Foundation of Transient Optics Technology (Grant No. YAK20006).

[1] Mordechai Segev, Bruno Crosignani, Amnon Yariv, and Baruch Fischer, Phys. Rev. Lett. **68**, 923 (1992).
[2] M. Segev, A. Yariv, B. Crosignani, P. DiPorto, G. Duree, G. Salamo, and E. Sharp, Opt. Lett. **19**, 1296 (1994).
[3] D. N. Christodoulides and M. I. Carvalho, Opt. Lett. **19**, 1714 (1994).
[4] M. Segev, G. C. Valley, Bruno Crosignani, Paolo Diporto, and Amnon Yariv, Phys. Rev. Lett. **73**, 3211 (1994).
[5] D. N. Christodoulides and M. I. Carvalho, J. Opt. Soc. Am. B **12**, 1628 (1995).
[6] S. R. Singh and D. N. Christodoulides, Opt. Commun. **118**, 569 (1995).
[7] M. Segev, M. Shih, and G. C. Valley, J. Opt. Soc. Am. B **13**, 706 (1996).
[8] M. D. Iturbe-Castillo, P. A. Marquez-Aguilar, J. J. Sanchez-Mondragon, S. Stepanov, and V. Vysloukh, Appl. Phys. Lett. **64**, 408 (1994).
[9] M. Shih, M. Segev, G. C. Valley, G. Salamo, B. Crosignani,

and P. DiPorto, Electron. Lett. **31**, 826 (1995); M.-F. Shih, P. Leach, M. Segev, M. H. Garrett, G. Salamo, and G. C. Valley, Opt. Lett. **21**, 324 (1996).
[10] G. C. Valley, M. Segev, Bruno Crosignani, Amnon Yariv, M. M. Fejer, and M. C. Bashaw, Phys. Rev. A **50**, R4457 (1994).
[11] M. Taya, M. Bashaw, M. M. Fejer, M. Segev, and G. C. Vally, Phys. Rev. A **52**, 3095 (1995).
[12] M. Taya, M. Bashaw, M. M. Fejer, M. Segev, and G. C. Valley, Opt. Lett. **21**, 943 (1996).
[13] M. Segev, George C. Valley, M. C. Bashaw, M. Taya, and M. M. Fejer, J. Opt. Soc. Am. B **14**, 1772 (1997).
[14] S. Bian, J. Frejlich, and K. H. Ringhofer, Phys. Rev. Lett. **78**, 4035 (1997).
[15] Charalambos Anastassiou, Ming-feng Shih, Matthew Mitchell, Zhigang Chen, and Mordechai Segev, Opt. Lett. **23**, 924 (1998).
[16] Minoru Taya, Matthew C. Bashaw, M. M. Fejer, Mordechai Segev, and George C. Valley, Opt. Lett. **21**, 943 (1996).
[17] Zhigang Chen, Mordechai Segev, Daniel W. Wilson, Richard E. Muller, and Paul D. Maker, Phys. Rev. Lett. **78**, 2948 (1997).
[18] Mordechai Segev, George C. Valley, S. R. Singh, M. I. Carvalho, and D. N. Christodoulides, Opt. Lett. **20**, 1764 (1995).
[19] M. I. Carvalho, S. R. Singh, D. N. Christodoulides, and R. I. Joseph, Phys. Rev. E **53**, R53 (1996).
[20] D. N. Christodoulides, S. R. Singh, M. I. Carvalho, and M. Segev, Appl. Phys. Lett. **68**, 1763 (1996).
[21] Zhigang Chen, Mordechai Segev, Tamer H. Coskun, and Demetrios N. Christodoulides, Opt. Lett. **21**, 1436 (1996).
[22] Zhigang Chen, Mordechai Segev, Tamer H. Coskun, Demetrios N. Christodoulides, and Vsevolod V. Afanasjev, Opt. Lett. **21**, 1821 (1996).
[23] Tamer H. Coskun, Demetrios N. Christodoulides, Young-Rae Kim, Zhigang Chen, Marin Soljacic, and Mordechai Segv, Phys. Rev. Lett. **84**, 2374 (2000).
[24] Nail Akhmediev, Wieslaw Krolikowski, and A. W. Snyder, Phys. Rev. Lett. **81**, 4632 (1998).
[25] Matthew Mitchell, Mordechai Segev, and Demetrios N. Christodoulides, Phys. Rev. Lett. **80**, 4657 (1998).
[26] Elena A. Ostrovskaya, Yuri S. Kivshar, Dmitry V. Skryabin, and William J. Firth, Phys. Rev. Lett. **83**, 296 (1999).
[27] Liu Jinsong and Lu Keqing, J. Opt. Soc. Am. B **16**, 550 (1999).
[28] Lu Keqing and Tang Tian-tong, Acta Phys. Sin. **48**, 2070 (1999).
[29] Lu Keqing, Tang Tiantong, and Zhang Yanpeng, Phys. Rev. A **61**, 053822 (2000).
[30] Marin Soljacic, Mordechai Segev, Tamer Coskun, Demetrios N. Christodoulides, and Ashvin Vishwanath, Phys. Rev. Lett. **84**, 467 (2000).